Design, development and validation of smart sensor drifting node with INSAT telemetry for oceanographic applications

Shijo Zacharia[1,*], R. Seshasayanan[2], R. Srinivasan[1], T. Thamarai[1], Tata Sudhakar[1], R. R. Rao[1] and M. A. Atmanand[1]

[1]National Institute of Ocean Technology, Ministry of Earth Sciences, Pallikaranai, Chennai 600 100, India
[2]College of Engineering, Guindy Campus, Anna University, Chennai 600 025, India

Drifter buoys are globally deployed to measure surface meteorological and oceanographic variables. A Lagrangian drifting buoy (Pradyu II) to measure sea-surface temperature and current has been developed at the National Institute of Ocean Technology, Chennai. The drifter buoy with geostationary satellite communication (INSAT-3C) to have near real-time data at every hour is a unique attempt in the history of drifting buoy nodes. This article describes Pradyu II drifting buoy node, design of low-power embedded system, communication network and field test results from an experiment conducted in the Bay of Bengal during March–April 2013. The results from Pradyu II are compared with commercially available drifting buoy (Marlin-Yug), moored data buoy (BD11) and remotely sensed data.

Keywords. Drifting buoy, embedded system, sea-surface temperature, sensor node.

ACCURATE knowledge on ocean circulation and air–sea interaction is essential to formulate a reliable ocean state prediction model. Tropical sea-surface temperature (SST) indicates the potential for atmospheric convection, heat exchange between ocean and atmosphere, biological productivity and climatic state. Ocean currents transfer heat from lower to higher latitudes. Hence SST and ocean currents have a significant impact on the world's weather and climate. Remote sensing satellites have been providing SST data with high spatial and temporal resolution for more than three decades[1,2]. Remote sensing of SST is limited by the presence of cloud and rain. Absolute values of SST are important to understand nonlinear relationship between atmospheric convection and ocean–atmosphere coupling[3]. The Lagrangian drifting floats are widely deployed to measure near-surface ocean currents[4,5]. The state-of-the-art electronics, improved communication technology, high energy power pack availability and advances in sensor technology have facilitated technologists to develop drifting buoys for long time observation with multiple sensors. A significant development of drifting buoys took place under the surface velocity programme (SVP) of the Tropical Ocean Global Atmosphere (TOGA) experiment and the World Ocean Circulation Experiment[6]. The Global Ocean Observation System (GOOS) programme deployed 1250 drifting buoys[7,8]. The drifting buoys are powered with internal battery and communicate over short-range radio frequency or through low-orbit satellites (POLAR, LEO).

A moored data buoy programme was initiated in India at the National Institute of Ocean Technology (NIOT), Chennai in 1997 and buoys were deployed in the Bay of Bengal and Arabian Sea[9]. In 2012, NIOT indigenized a drifting buoy (Pradyu I)[10,11].

This article describes a unique attempt with 96 temperature measurements per day, 24 GPS position acquisitions per day and geostationary satellite communication to have near real-time data at every hour using the drifting buoy. The drifting buoy is capable of measuring fluctuations in SST and small-scale surface eddies. This article also describes details of Pradyu II drifting buoy node, design of low-power embedded system and network architecture. The field test results of Pradyu II in the Bay of Bengal experiment in summer 2013 are validated with data from a commercially available drifting buoy (Marlin-Yug) deployed along with it, data from a nearby moored data buoy (BD11) and remotely sensed Advanced Very High Resolution Radiometer (AVHRR) satellite data.

Sensor node description

The drifting buoy node is made of a flanged two-part spherical float of 0.4 m diameter made of epoxy resins. A detailed schematic of the drifting buoy is shown in Figure 1. The bottom half of the float houses a battery pack, embedded system, power control switch, power control circuits and satellite modem. The node is equipped with SST sensor and a GPS. The bottom half of the sphere is coated with antifouling paint. The upper half of the float is covered with ultraviolet protective coating. A 12 m

*For correspondence. (e-mail: zacharia@niot.res.in)

stainless steel tether wire is connected to an eye bolt at the bottom centre of the float. The bottom centre area of the float is strengthened internally. The bottom end of the tether is attached to a disc-type frame on windowed cylindrical holy sock drogue. The drogue has PVC ribs to keep it circular. A photograph of the drifting buoy and drogue is shown in Figure 2.

The system block diagram of the node is shown in Figure 3. It comprises of an embedded system, GPS module, SST sensor ($SST_{P0.16}$) on the bottom half of the hull at 0.16 m below water level, solid-state power control circuits, reed relay and a battery pack.

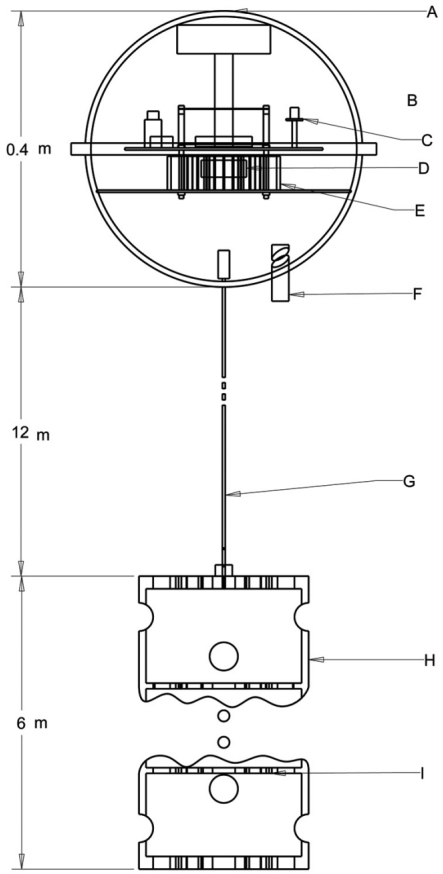

Figure 1. Schematic of drifting buoy and drogue. (A, Hull; B, INSAT modem and GPS; C, Controller PCB; D, Magnetic relay; E, Power Pack; F, SST; G, SS tether; H, Drogue; I, PVC ribs.)

Figure 2. Pradyu II drifter buoy and its drogue.

Network architecture

Drifting buoys are mobile nodes with global communication coverage. A single-hop communication link between the drifting buoy node and satellite establishes the network link. The drogue on the drifting buoy is subjected

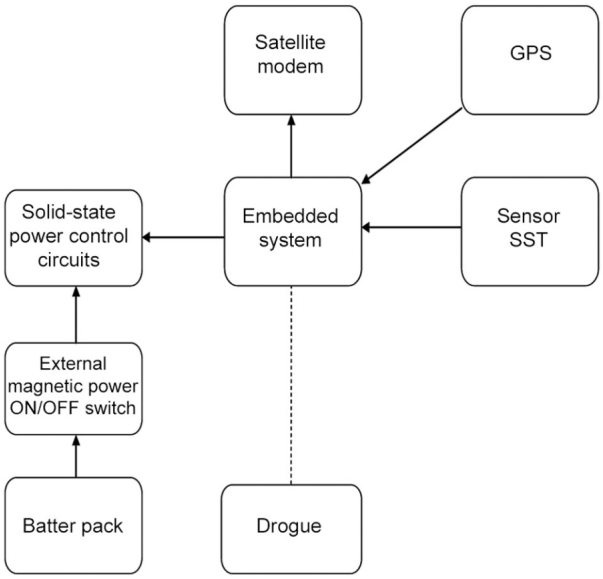

Figure 3. System block diagram.

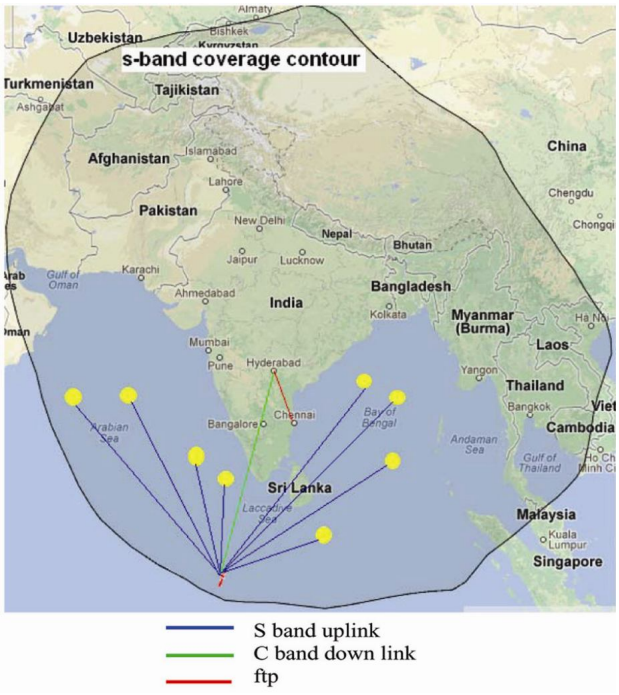

Figure 4. Network architecture.

to ocean currents and it provides mobility. The drifting buoy network is expandable for wide spatial coverage. Each node has a GPS to measure its position and maintains real time clock (RTC). The nodes communicate periodically in TDMA mode to the geostationary INSAT satellite at 2.6 GHz frequency. The satellite down-links the data at 4.3 GHz to the Earth station at Hyderabad, India. The Earth station is connected to the data reception system at NIOT, Chennai. A schematic view of the network architecture is shown in Figure 4.

Controller

A conventional micro-controller needs to be integrated with external analogue and digital discrete components to build a sensor node[12,13]. Programmable System On Chip (PSOC) is a reconfigurable, embedded, mixed signal programmable system on chip manufactured by Cypress Semiconductor, USA[14]. The PSOC Integrated Chip (IC) has built-in programmable analogue and digital blocks to implement peripherals on requirement. The PSOC can be programmed to replace fixed function ICs, microcontrollers and ASIC. Power consumption of the system can be reduced by programming on-board peripherals in sleep mode in PSOC-embedded controller. In this article we report the design of a battery-powered PSOC embedded system for ultra-low power application. In the present application digital peripherals such as UART, RTC, clock divider, RAM memory, digital IO, eight-bit microcontroller and analogue peripherals such as voltage reference, current source, operational amplifier, oscillator, analogue multiplexer and analogue-to-digital converter are implemented on a single chip. The PSOC consumes only 0.8 mA@ 3 MHz at 5 V in active mode and 1 μA in sleep mode with RTC in 'on' state. In order to keep the RTC active a sleep mode with wake up using 1 sec RTC timer is adopted. Reducing steady-state power consumption of the system by 1 mA may result in saving of 8.8 Ah annually. Considering the above aspects, PSOC is an ideal choice for sensor node controller[15]. The schematic of internal peripherals (IO, three UARTs, RTC and 5 Hz clock source) is shown in Figure 5. Three on-board UARTs are configured for interfacing with the INSAT satellite modem, GPS and host port interface. The embedded controller controls subsystem power, measures SST at every one minute interval, averages 15 min data, acquires geographic position from GPS at every hour and communicates to the data reception centre through INSAT satellite telemetry.

Sensors

SST sensor: A four-wire negative temperature coefficient-type thermistor circuit is used to measure temperature. A reference resistor method is adopted to make the measurement independent of offset error. In this method a programmable current source (i_{DAC}) excites series combination of reference resistance R_{STD} and thermistor (Omega 44005, R_T). The schematic of temperature measurement method is shown in Figure 6. The power is applied to the $SST_{P0.16}$ sensor only for 100 ms during measurement. In the offset measuring state, the current source inside the PSOC is programmed to give 0 μA and the series branch of resistors is connected to the reference to measure offset error.

In offset measuring state:

$$i_{DAC(t)} = 0, \quad v_{0(t)} = i_{DAC(t)} \times R_{STD} + v_{ADC0(t)}, \tag{1}$$

$$i_{DAC(t')} = 0, \quad v_{1(t')} = i_{DAC(t')} \times R_T + v_{ADC1(t')}. \tag{2}$$

$v_{ADC0(t)}$ and $i_{ADC1(t')}$ are combined offset of multiplexer and Analogue to Digital Converter (ADC) for channels 0 and 1 respectively. In resistance measurement state, the

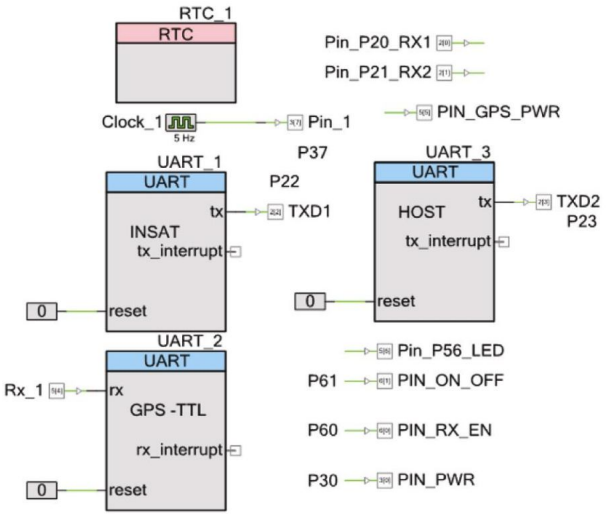

Figure 5. Schematic diagram of internal peripherals of PSOC IC.

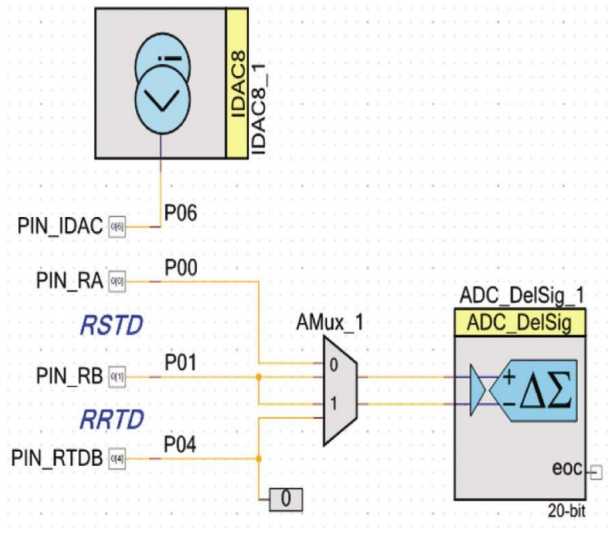

Figure 6. Schematic diagram of temperature measurement circuit.

current source is set to 15 μA and voltage across R_{STD} and R_{RTD} is measured.

In resistance measurement state

$$v_{0(t'')} = i_{DAC(t'')} \times R_{STD} + v_{ADC0(t'')}, \quad (3)$$

$$v_{1(t''')} = i_{DAC(t''')} \times R_T + v_{ADC1(t''')}. \quad (4)$$

Since t, t', t'', t''' are very close events,

$$v_{ADC0(t''')} = v_{0(t)} \text{ and } v_{ADC1(t''')} = v_{1(t')}.$$

Now,

$$R_T = \frac{v_{1(t''')} - v_{1(t')}}{\left(\frac{v_{0(t'')} - v_{0(t)}}{R_{STD}}\right)}, \quad (5)$$

where v_{ADC0} and v_{ADC1} are voltages across R_{STD} and R_T respectively.

The R_{STD} resistor is a precision resistor with temperature coefficient of resistance 10 ppm/°C and 0.01% tolerance. The $SST_{P0.16}$ probe is calibrated for temperature range from 20°C to 35°C in an oil temperature bath at NABL accredited facility. A best-fit curve is derived from the calibration result and is given in eq. (6).

$$T(°C) = -23.9 \times \ln(R_T) + 51.44. \quad (6)$$

It is implemented in the firmware for automated measurement.

It is evident that this measurement scheme nulls the offset error in multiplexer and ADC, but reduces sampling frequency by one-fourth. An in-built 20-bit ADC in PSOC measures multiplexed voltages.

GPS: A GPS receiver module with 65 channels at L1 frequency of 1575.42 MHz coarse acquisition code provides positional information and time synchronization. The GPS has circular error probability of 2.5 m radius. The GPS receiver is normally in 'off' state and is switched on for 60 sec and position is captured in the next 60 sec. The power to the GPS is switched off after position and time acquisition. The GPS module is interfaced to controller module through RS232 TTL interface in National Marine Electronic Association (NMEA), 4800 bps protocol.

Power pack

A power pack of 24Ah@0.75A with nominal voltage of 24 V is made of series–parallel combination of 32 numbers of 1.5 V D-size alkaline LR20 cells (MN1300, Duracell). Tin-coated stainless steel strips are laser-welded to the cell terminals to establish connectivity. The parallel branches are connected through reverse protection diodes.

Power control

An external magnet activates a reed switch fixed inside the buoy hull and disconnects the power pack. Power to the sensors and satellite modem is controlled through MOSFET switch. With power on, the PSOC controller enters the sleep mode and is activated by a 1 Hz trigger from RTC. The $SST_{P0.16}$ sensor, GPS and satellite modem are in 'off' state normally. The PSOC controller measures temperature at every minute. The sensor power control scheme is shown in Table 1.

Communication

The INSAT-3C satellite mission is to support communication, broadcasting and meteorology services[16]. The satellite is located in 74°E longitude. It is equipped with 24 C-band transponders, six extended C-band transponders and two S-band transponders[17–19].

The satellite modem of Pradyu II drifting buoy uplinks BPSK modulated data in S-band. The transmission slot of each sensor node is disciplined at a specific time slot

Table 1. Sensor power control scheme

Time (min)	GPS	Satellite modem	$SST_{P\,0.2}$
58	On	Off	On for 100 ms
59	Position measurement	On	On for 100 ms
60	Off	Data transmission	On for 100 ms
1	Off	Data transmission	On for 100 ms
2 to 57	Off	Off	On for 100 ms

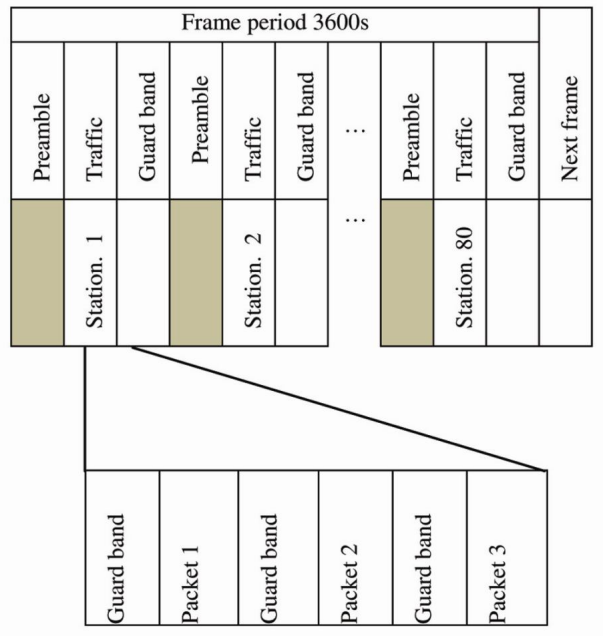

Figure 7. TDMA frame structure.

(TDMA). The data are transmitted at 300 bps in burst mode. The TDMA frame period is 60 min with 80 stations[20]. The TDMA frame structure is shown in Figure 7. A 52-byte packet is transmitted in 2.7 sec in burst mode. The drifting buoys are often dipped in water in wave action. The node repeatedly transmits two more packets in a slot to improve the data reliability in case of wave action. The satellite transmitter consumes 41 mA in standby mode, 335 mA in active mode and 2.1 A during burst transmission at 24 Vdc. It operates from 11.5 Vdc to 25 Vdc. The INSAT MSS terminal and controller is interfaced through RS232 serial port. The terminal has been developed by Indian Space Research Organisation (ISRO) and manufactured by Avantel Limited[21].

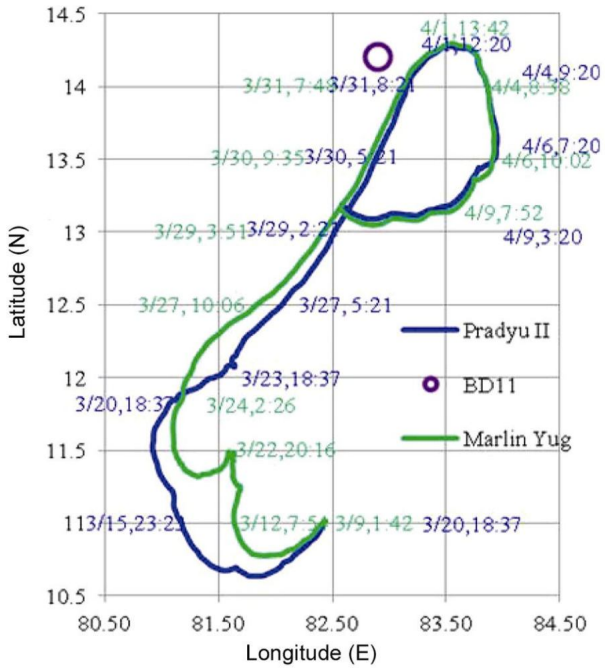

Figure 8. Trajectories of drifting buoys and position of BD11.

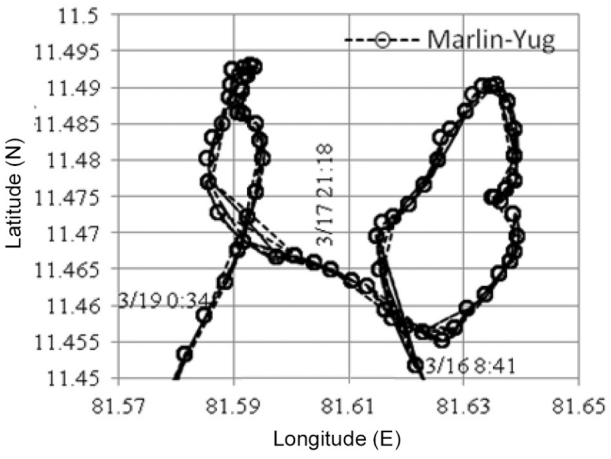

Figure 9. Detailed trajectory of Marlin-Yug drifting buoy from 16 to 19 March 2013.

The satellite Earth station is located at Hyderabad. The automated Earth station transfers data through ftp to the NIOT server in Chennai.

Field test

Materials and methods

The Pradyu II and Marlin-Yug drifting buoys were deployed by availing ocean research vessel, *ORV Sindhu Sankalp* on 8 March 2013 at 16 : 39 : 00 h at 11.0867N, 82.033E in the Bay of Bengal. Both Pradyu II and Marlin-Yug drifting buoys have the same drift characteristics. They have SST sensors at 0.16 m below water level. The Pradyu II drifting buoy measures SST ($SST_{P0.16}$) temperature at every minute and 15 min average temperatures are transmitted. It transmits GPS position at every hour interval. Pradyu II transmits 96 (15 min averaged) temperature and 24 position data daily. It communicates at every hour in real time through geosynchronous

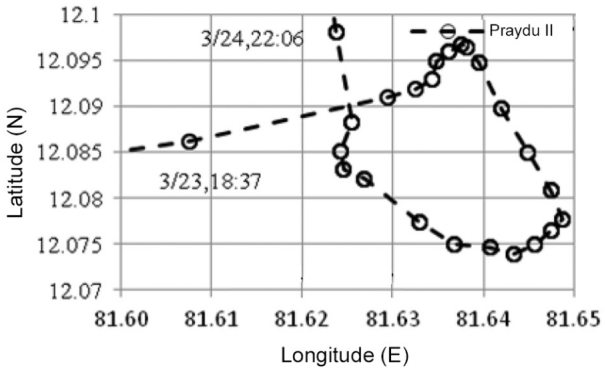

Figure 10. Trajectory of Pradyu II drifting buoy during 23–24 March 2013.

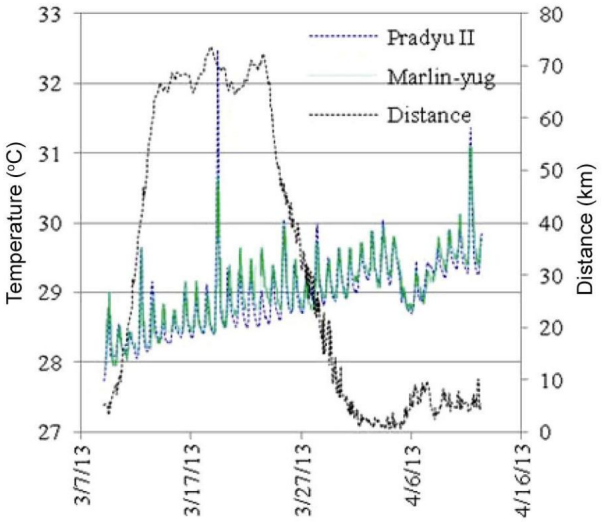

Figure 11. Distance between Pradyu II and Marlin-Yug drifting buoys and their sea-surface temperature time series.

INSAT in S-band. The Marlin-Yug drifting buoy transmits only 4–5 SST ($SST_{M\,0.16}$) values and position data daily. The trajectories, drifting speeds and SST of Pradyu II have been compared with Marlin-Yug.

The $SST_{P0.16}$ has been compared with SSTs ($SST_{BD11\,1}$, $SST_{BD11\,5}$) of moored buoy BD11 (at 14.203N, 82.93E) from 9 March to 12 April 2013. The daily mean SST measured by Pradyu II and that over the region of study measured with AVHRR on remote sensing satellite have also been compared from 9 March to 12 April 2013.

Distance and drift speed calculation

The distance $\delta(t)$ between successive reported positions $x(t)$ and $x(t')$ are calculated using the haversine formula, where $x(t) = (\alpha, \beta)$ and $x(t') = (\alpha', \beta')$, α and α' are latitudes of positions and, β and β' are longitudes of positions.

$$a = \sin\left(\frac{|\alpha - \alpha'| \times \pi}{180 \times 2}\right)^2 + \cos\left(\frac{\alpha \times \pi}{180}\right) \times \cos\left(\frac{\alpha' \times \pi}{180}\right) \times \sin\left(\frac{|\beta - \beta'| \times \pi}{180 \times 2}\right)^2, \quad (7)$$

$$\delta(t) = 2 \times 6371 \times \arctan(\sqrt{a}, \sqrt{(1-a)})\,(\text{km}). \quad (8)$$

The drift speed between t and t' is

$$s(t) = \frac{\delta(t)}{t - t'}\ (\text{km s}^{-1}). \quad (9)$$

Results and discussion

Comparison of trajectories of Pradyu II and Marlin-Yug drifting buoy

The trajectories of the drifting buoys from 9 March to 12 April 2013 and BD11 position are shown in Figure 8. Due to a time lag of 10 min in the deployment and local surface turbulence, the drifting buoys initially followed dissimilar trajectories in the same direction. The Marlin-Yug drifting buoy followed a clockwise north–south elliptical eddy on 16 and 17 March 2013 with a major and minor axis of 4.2 and 2.7 km respectively. The Marlin-Yug drifting buoy mapped in a second similar eddy on 17–19 March 2013 with a major and minor axis of 2.6 and 1 km respectively. The detailed trajectory and time stamp of Marlin-Yug drifting buoy from 16 to 19 March 2013 are shown in Figure 9. The Pradyu II drifting buoy is wafted to position 11.8716N, 81.106E on 20 March 2013 at 18 : 37 : 00 h, but Merlin-Yug drifting buoy arrived there only on 24 March 2013 at 15 : 03 : 42 h. The two clockwise elliptical eddies of Marlin-Yug drifting buoy made its position towards south compared to Pradyu II in the initial trajectory. The drifting buoys followed a similar trajectory from the above position, except a north–south clockwise elliptical eddy with major axis 2.6 km and minor axis 2.3 km made by Pradyu II drifting buoy during 23 and 24 March 2013. In this section the Marlin-Yug drifting buoy followed the trajectory of Pradyu II within 1–4 h. The detailed trajectory and time stamp of Pradyu II drifting buoy in the above period are shown in Figure 10. The maximum observed distance between the trajectories is 73.7 km and the minimum is 0.4 km. The distance between two drifting buoys with respect to time is shown in Figure 11. Even though both the buoys drifted in neighbouring distinct trajectories with 1–4 h delay, they intersected again at 14.16N, 83.78E on 4 April 2013 and at 13.51N, 83.91E on 6 April 2013. The drifting buoys had undergone a clockwise east-south

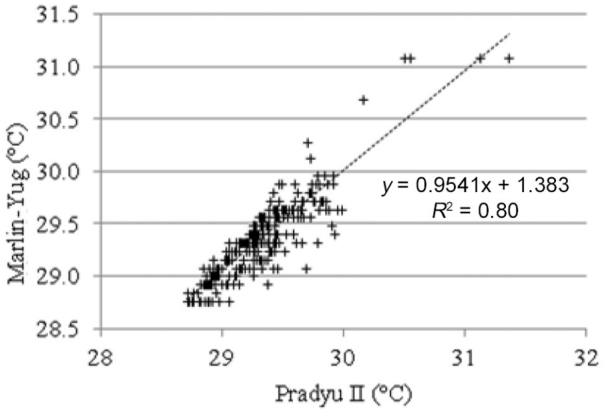

Figure 12. Comparison of sea-surface temperature of Pradyu II and Marlin-Yug drifting buoys from 28 March to 12 April 2013.

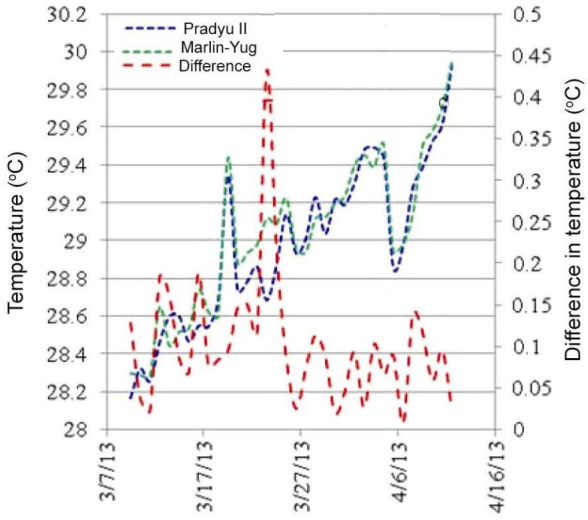

Figure 13. Daily average sea-surface temperature of Pradyu II and Marlin-Yug drifting buoys.

semicircular trajectory of 146 km diameter from 29 March to 12 April 2013.

Comparison of SST measured by Pradyu II and Marlin-Yug drifting buoys

The SSTs measured by Pradyu II ($SST_{P\ 0.16}$) and Marlin-Yug ($SST_{M0.16}$) drifting buoys are shown in Figure 11. It is observed that the both measurements are strongly correlated with coefficient of determination R^2 value of 0.80 when their trajectories are separated less than 25 km from 28 March to 12 April 2013. The scatter plot of SST of the drifting buoys for the above period is presented in Figure 12.

The daily average SSTs of the drifting buoys are post-processed. The daily average temperature and the absolute difference of the drifting buoys are shown in Figure 13. The absolute difference of daily average temperatures of the drifting buoys is less than 0.15°C, when they are separated less than 25 km for the period from 28 March to 12 April 2013. It is observed that the daily average SST of both the drifting buoys is strongly correlated with coefficient of determination R^2 value of 0.93. The scatter plot of SSTs of the drifting buoys for the above period is presented in Figure 14.

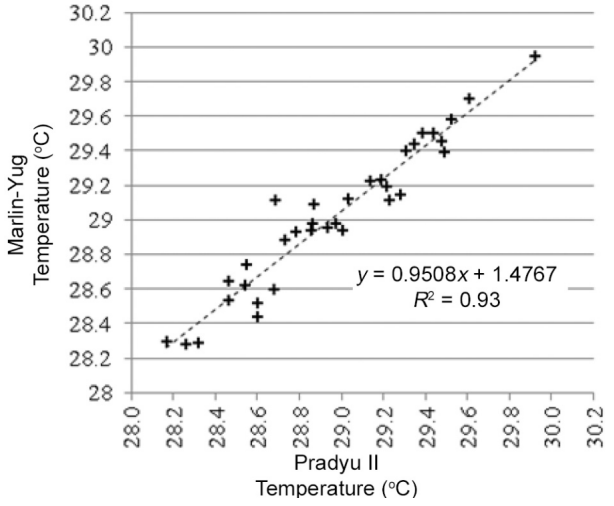

Figure 14. Scatter plot of daily average sea-surface temperature of Pradyu II and Marlin-Yug drifting buoys.

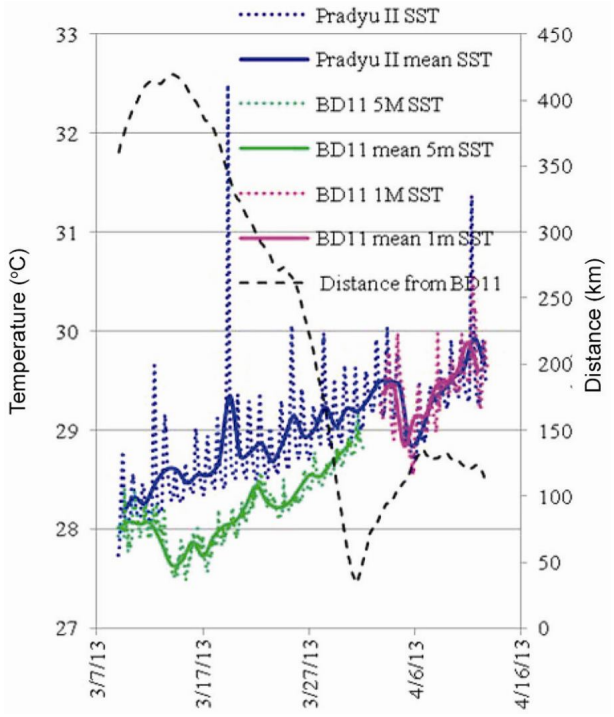

Figure 15. Comparison of sea-surface temperature of Pradyu II and BD11.

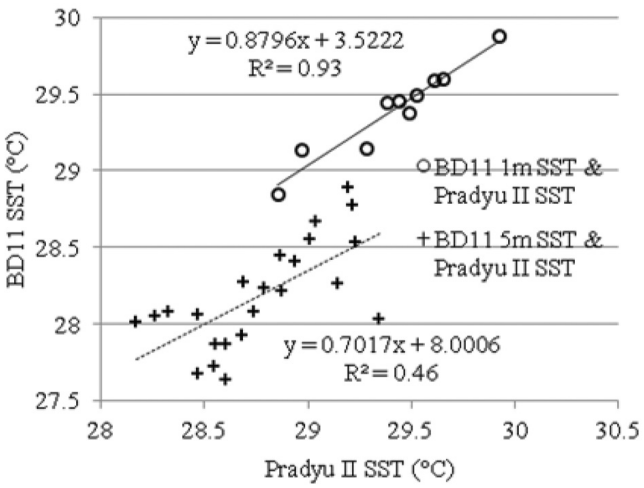

Figure 16. Scatter plots of daily average sea-surface temperature of Pradyu II and BD11.

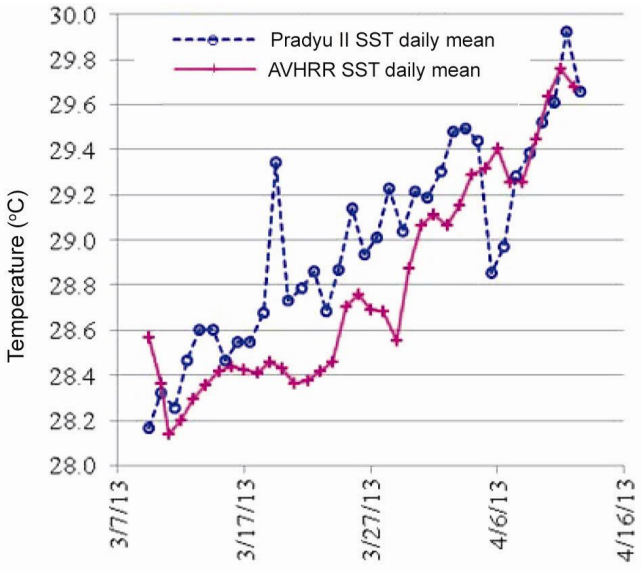

Figure 17. Daily average of Pradyu II sea-surface temperature and AVHRR SST.

Comparison of SST measured by Pradyu II and moored buoy (BD11)

The drifting buoys were floated within 419 km from the moored buoy BD11 for the period from 9 March to 12 April 2013. They were at a distance of only 35 km away from BD11 on 31 March 2013. The data buoy BD11 is equipped with SST sensors at 1 m ($SST_{BD11\,1}$) and 5 m ($SST_{BD11\,5}$) below water level. The BD11 measures $SST_{BD11\,1}$ once in 3 h and $SST_{BD11\,5}$ every hour. Pradyu II measures $SST_{P0.16}$ at every 15 min interval.

The time series of $SST_{P0.16}$ of the drifting buoy, $SST_{BD11\,1}$, $SST_{BD11\,5}$ and their daily mean values along with distance between BD11 and Pradyu II drifting buoy are shown in Figure 15. A warming of the ocean from 28.17°C to 29.21°C is observed in $SST_{P0.16}$ and 28.01°C to 28.89°C is recorded in $SST_{BD11\,5}$ during 9–31 March 2013. The diurnal amplitude of SST is relatively larger in $SST_{P0.16}$ (sensor depth 0.16 m) compared to corresponding amplitude observed by $SST_{BD11\,5}$ (sensor depth 5 m), which is in agreement with earlier studies[22–26]. A maximum difference of 1.31°C is observed as the distance between Pradyu II and BD11 varied from 47 to 416 km during the above period. The scatter plots of daily average temperatures $SST_{P0.16}$ and $SST_{BD11\,5}$ are shown in Figure 16. A moderate correlation with coefficient of determination R^2 value of 0.46 exists between them.

Notably, during 3–12 April 2013 although Pradyu II and BD11 were apart by 97–130 km, daily mean of $SST_{P0.16}$ and $SST_{BD11\,1}$ shows very strong agreement in absolute and temporal trend with a coefficient of determination R^2 value of 0.93. The scatter plots of average temperatures are shown in Figure 16. The drifting nature of Pradyu II reveals a typical spatial variation of SST that is seen in this region. It is suggested that the discrepancy between SST measured by Pradyu II and BD11 could be partly a manifestation of the variation of temperature with depth in the surface layer[27]. The buoy BD11 measurements were occasionally overestimated than Pradyu II significantly due to difference between skin and bulk temperatures[9,28].

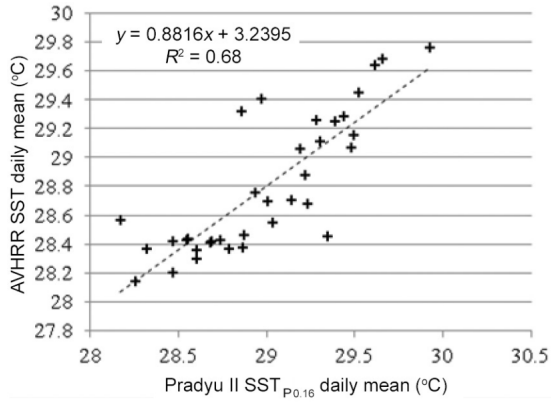

Figure 18. Scatter plot of daily average sea-surface temperature of Pradyu II and AVHRR.

Comparison of SST measured by Pradyu II and AVHRR

The daily average SST of Pradyu II and remote-sensed data measured by AVHRR over the region 10.5–14.5N, 80.5–84.5E, is compared from 9 March to 12 April 2013 (ref. 29). The daily average temperatures are shown in Figure 17. The Pradyu II and AVHRR measured a warming of the ocean about 1.6°C during this period. Direct comparison of daily mean of SSTs of Pradyu II and AVHRR has shown good agreement with a coefficient of determination R^2 value of 0.68. A scatter plot of the comparison is shown in Figure 18. The difference between Pradyu II and AVHRR is less than 0.9°C in the daily mean SST (Pradyu II is warmer). The AVHRR SST corresponds to the top 10 μm or so, whereas the Pradyu II SST is at 0.16 m below the surface. The difference between the above measurements could be partly due to difference in sensing depth and atmospheric effects[27,30,31].

Comparison of drift speeds of Pradyu II and Marlin-Yug drifting buoys

The daily drift speeds of drifting buoys are derived using eqs (7)–(9). The drift speeds of Pradyu II and Marlin-Yug drifting buoys and distance between them are shown in Figure 19. It is observed that typical spatial variations of currents measured by the drifting buoys are less than 0.15 m/s within 40 km range. A maximum spatial variation of current measured by the drifting buoys is 0.4 m/s in 70 km range.

A scatter plot of current derived from the positions of the drifting buoys from 25 March to 12 April 2013 is shown in Figure 20. A strong agreement of current measurements is seen with coefficient of determination R^2 value of 0.88 over the region when the buoys were separated by less than 40 km.

Conclusion

The design details of indigenous Pradyu II drifting buoys are reported here. A sensor node with low-power PSOC embedded controller for temperature and position measurement is depicted. A geosynchronous INSAT-3C satellite communication is implemented in drifting buoy node for wide spatial coverage of network and near real-time communication.

The SST and drift speed of Pradyu II and Marlin-Yug drifting buoys are compared for the period 9 March to 12 April 2013. It is observed that the daily average SST of both drifting buoys is strongly correlated with coefficient

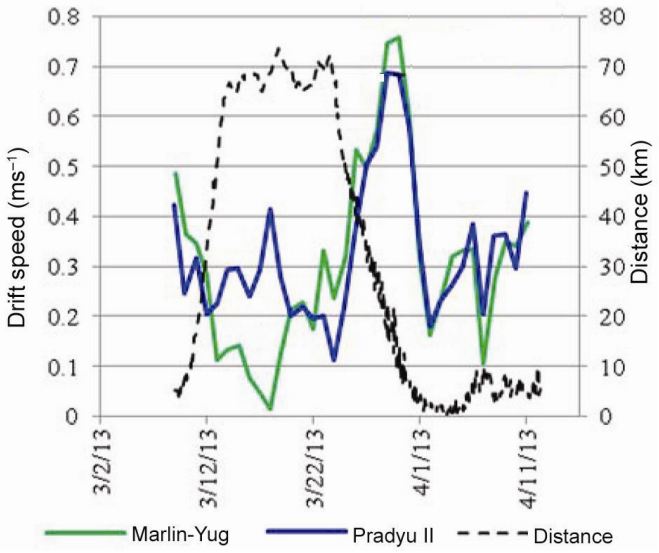

Figure 19. Drift speed of Pradyu II and Marlin-Yug drifting buoys.

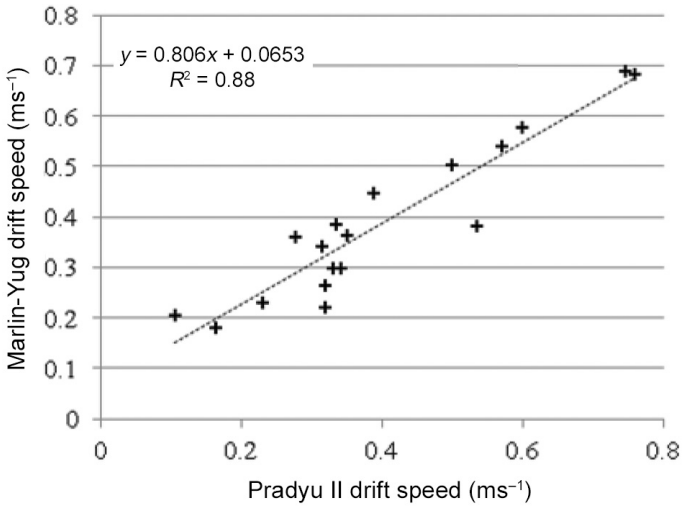

Figure 20. Scatter plot of current derived from the positions of Pradyu II and the Marlin-Yug drifting buoys.

of determination R^2 value of 0.93. A strong agreement of current measurements is seen with coefficient of determination R^2 value of 0.88 over the region, when the buoys were separated by less than 40 km.

The daily mean $SST_{P0.16}$ and $SST_{BD11\ 1}$ shows strong agreement in absolute and temporal trend with a coefficient of determination R^2 value of 0.93. The direct comparison of daily mean SST of Pradyu II and AVHRR is strong with coefficient of determination R^2 value of 0.68.

Warming of the ocean from about 28.17°C to 29.92°C is observed in the Pradyu II drifting buoy data and is in strong agreement with other *in situ* measurements and remote sensing. Higher sampling rate (96 samples/day) helped Pradyu II to detect prominent SST peaks. The measurement scheme with 24 GPS position acquisitions per day is capable of measuring smaller surface eddy with major axis 2.6 km and minor axis 2.3 km (on 23 March 2013).

More work is needed to understand the nature of the ocean and its spatial and temporal variations.

1. Epstein, E. S., Callicott, W. M., Cotter, D. J. and Yates, H. W., NOAA satellite programs. *IEEE Trans. Aerosp. Electron. Syst.*, 1984, **AES-20**(4), 325–344.
2. Koffler, R., Use of NOAA environmental satellites to remotely sense ocean phenomena. In OCEAN 1975 Conference, San Diego, USA, 1975, pp. 835–839; doi:10.1109/OCEANS.1975.1154116.
3. Bjerknes, J., Atmospheric teleconnections from the equatorial Pacific. *Mon. Weather. Rev.*, 1969, **97**, 163–172.
4. Smith, P., Frye, D. and Cresswell, G., New low-cost ARGOS drifting buoy. Oceans Conference, Washington DC, USA, 1984, pp. 745–747; doi: 10.1109/OCEANS.1984.1152276.
5. Lanza, M., A low-cost expendable Loran-based drifting buoy. Oceans Conference, Washington DC, USA, 1984, pp. 741–744; doi:10.1109/OCEANS.1984.1152286.

6. http://woce.nodc.noaa.gov/wdiu/ (accessed on 15 August 2013).
7. http://www.ioc-goos.org/index.php?option=com_content&view=article&id=297%3Adrifting-buoys&catid=60%3Aobserving-systems&Itemid=100097&lang=en (accessed on 15 August 2013).
8. Soreide, N. N., Woody, C. E. and Holt, S. M., Overview of ocean based buoys and drifters: present applications and future needs. Oceans, MTS/IEEE Conference and Exhibition, 2001, vol. 4, 2470–2472; doi: 10.1109/OCEANS.2001.968388.
9. Premkumar, K., Ravichandran, M., Kalsi, S. R., Sengupta, D. and Gadgil, S., First results from a new observational system over the Indian seas. *Curr. Sci.*, 2000, **78**, 323–331.
10. Srinivasan, R., Zacharia, S., Sudhakar, T., Thamarai, T., Gowthaman, V. and Atmanand, M. A., A smart sensor drifting buoy node with INSAT communication for meteorological and oceanographic applications. Patent application no 400/CHE/2013 dated 30/01/2013.
11. Sudhakar, T. *et al.*, Detection of sea-surface temperature anomaly in the equatorial region of Bay of Bengal using indigenous Lagrangian drifter. *Curr. Sci.*, 2013, **104**(2), 177–178.
12. Sohraby, K., Minoli, D. and Taiebznati, I., *Wireless Sensor Network Technology, Protocols and Applications*, Wiley, 2006, pp. 75–78.
13. Karl, H. and Willing, A., *Protocols and Architectures for Wireless Sensor Networks*, Wiley India (P) Ltd, 2005, pp. 17–32.
14. http://www.cypress.com/psoc/ (accessed on 15 August 2013).
15. Mohiddin, R. *et al.*, Building a sensor network with PSoC. In Fifth International Conference on Sensing Technology (ICST), Palmerston North, 2011, pp. 353–357; doi: 10.1109/ICSensT.2011.6136997.
16. http://www.isro.org/satellites/insat-3c.aspx (accessed on 15 August 2013).
17. http://www.satbeams.com/footprints?beam=5670 (accessed on 15 August 2013).
18. Ghose, A. and Vasant, J., Mobile and portable communication using INSAT satellite. In IEEE International Conference on Personal Wireless Communications, New Delhi, 1996, pp. 301–306; doi: 10.1109/ICPWC.1996.494288.
19. Bandyopadhyay, K. and Venugopal, D., Personal messaging through INSAT-MSS. IEEE International Conference on Personal Wireless Communications, New Delhi, 1996, pp. 294–300; doi: 10.1109/ICPWC.1996.494287.
20. Pratt, T., Bostian, C. and Allnutt, J., *Satellite Communication*, Wiley India Edition, 2008, pp. 233–246.
21. http://www.isro.gov.in/ttg/pdfuploads/MSS_Type_D-Terminal.pdf (accessed on 15 August 2013).
22. Shenoi, S. S. C., Nasnodkar, N., Rajesh, G., Jossia Joseph, K., Suresh, I. and Almeida, A. M., On the diurnal ranges of sea surface temperature (SST) in the north Indian Ocean. *J. Earth Syst. Sci.*, 2009, **118**(5), 483–496.
23. Price, J. F., Weller, R. A. and Pinkel, R., Diurnal cycling: observations and models of upper ocean response to diurnal heating, cooling, and wind mixing. *J. Geophys. Res.*, 1986, **91**, 8411–8427.
24. Webster, P. J., Clayson, C. A. and Curry, J. A., Clouds, radiation, and the diurnal cycle of sea surface temperature in the tropical western Pacific. *J. Climate*, 1996, **9**, 1712–1730.
25. Weller, R. A. and Anderson, S. P., Surface meteorology and air–sea fluxes in the western equatorial Pacific warm pool during the TOGA coupled ocean–atmosphere response experiment. *J. Climate*, 1996, **9**, 1959–1990.
26. Kawai, Y. and Wada, A., Diurnal sea surface temperature variation and its impact on the atmosphere and ocean, a review. *J. Oceanogr.*, 2007, **63**, 721–744.
27. Wentz, F. J., Gentemann, C., Smith, D. and Chelton, D., Satellite measurements of sea surface temperature through clouds. *Science*, 2000, **288**, 847–850.
28. Donlon, C. J., Nightingale, T. J., Sheasby, T., Turner, J., Robinson, I. S. and Emery, W. J., Implications of the oceanic thermal skin temperature deviation at high wind speed. *Geophys. Res. Lett.*, 1999, **26**, 2505–2508.
29. http://las.incois.gov.in (accessed on 30 August 2013).
30. Park, K.-A., Lee, E.-Y., Chung, S.-R. and Sohn, E.-H., *Korean J. Remote Sensing*, 2011, **27**(6), 663–675.
31. Bhat, G. S., Vecchi, G. A. and Gadgil, S., Sea surface temperature of the Bay of Bengal derived from the TRMM microwave imager. *J. Atmos. Ocean. Technol.*, 2004, **21**, 1283–1290.

ACKNOWLEDGEMENTS. We thank the Ministry of Earth Sciences, Government of India for funds; Dr P. S. Rao, National Institute of Oceanography, Goa, for providing the ship for deployment of the drifting buoys, and staff of the Ocean Observation Group, NIOT, Chennai for sharing BD11 data. We also thank INCOIS for providing AVHRR data service in Live Access Server.

Received 20 November 2013; accepted 13 January 2014